OXFORD

Cerebral Cortex, 2023, **33**, 8748–8758
https://doi.org/10.1093/cercor/bhad156
Advance access publication date 17 May 2023
Original Article

Early threat perception is independent of later cognitive and behavioral control. A virtual reality-EEG-ECG study

Juanzhi Lu, Selma K. Kemmerer, Lars Riecke, Beatrice de Gelder*

Department of Cognitive Neuroscience, Faculty of Psychology and Neuroscience, Maastricht University, Maastricht 6200 MD, The Netherlands

*Corresponding author: Department of Cognitive Neuroscience, Faculty of Psychology and Neuroscience, Maastricht University, P.O. Box 616, 6200 MD, Maastricht, The Netherlands. Email: b.degelder@maastrichtuniversity.nl

Research on social threat has shown influences of various factors, such as agent characteristics, proximity, and social interaction on social threat perception. An important, yet understudied aspect of threat exposure concerns the ability to exert control over the threat and its implications for threat perception. In this study, we used a virtual reality (VR) environment showing an approaching avatar that was either angry (threatening body expression) or neutral (neutral body expression) and informed participants to stop avatars from coming closer under five levels of control success (0, 25, 50, 75, or 100%) when they felt uncomfortable. Behavioral results revealed that social threat triggered faster reactions at a greater virtual distance from the participant than the neutral avatar. Event-related potentials (ERPs) revealed that the angry avatar elicited a larger N170/vertex positive potential (VPP) and a smaller N3 than the neutral avatar. The 100% control condition elicited a larger late positive potential (LPP) than the 75% control condition. In addition, we observed enhanced theta power and accelerated heart rate for the angry avatar vs. neutral avatar, suggesting that these measures index threat perception. Our results indicate that perception of social threat takes place in early to middle cortical processing stages, and control ability is associated with cognitive evaluation in middle to late stages.

Key words: control success; electroencephalography; social threat; virtual reality.

Introduction

The ability to detect threat and react adaptively is a major evolutionary endowment of many species (LeDoux and Daw 2018). Human and non-human studies of defensive behavior have documented different kinds of behavior in the face of threat, mainly freezing and fleeing (Eilam 2005). Freezing has been defined as a threat-anticipatory state whereby an individual is hyperattentive to an environmental, potentially threatening signal, presumably also enhancing its processing (Blanchard et al. 1986; Mobbs and Kim 2015; Terburg et al. 2018; Livermore et al. 2021). Previous work has investigated freezing-like reactivity using threat-related social stimuli, such as facial expressions and affective films (Roelofs et al. 2010; Stins et al. 2011; Hagenaars et al. 2014), as well as computer-based tasks (e.g. a gun shooting task) (Gladwin et al. 2016) and most recently whole body expression (de Gelder et al. 2010; de Borst and de Gelder 2022; Mello et al. 2022). Bradycardia, a reduction in one's heart rate, and reduced postural mobility are two principal physiological components of the freezing state in the face of threats (Roelofs et al. 2010). This pattern of physiological and behavioral activation is especially coordinated by the subcortical connections between amygdala nuclei—the basolateral nucleus receiving multisensory information and the central nucleus sending the main projections out—and the periaqueductal gray, the hypothalamus, and the rostral ventrolateral medulla (George et al. 2019). Stimulation of this circuit activates the sympathetic and parasympathetic nervous systems, which in turn coordinate switches from passive defensive states (e.g. freezing) to active defensive behavior (e.g. flight or fight) (Terburg et al. 2018; Livermore et al. 2021).

A critical factor for freezing-like reactions in humans is the proximity of the threat. Studies on peripersonal space (PPS), the proximate space surrounding the body where interactions with environmental stimuli occur (Di Pellegrino and Làdavas 2015; Bufacchi and Iannetti 2018; Serino 2019), have shown that personal distance is an important determinant of defensive behavior in social interactions (Graziano and Cooke 2006; Brozzoli et al. 2013; Cléry et al. 2015; Pellencin et al. 2018; Bogdanova et al. 2021). The defensive reactivity to potentially threatening stimuli near the PPS is associated with reduced motor cortex excitability (Avenanti et al. 2012), increased physiological reactivity (Ruggiero et al. 2021), and enhanced neural processing of the target stimulus in brain regions involved in defensive behavior (Vieira et al. 2020). Moreover, the neural network underlying PPS has been shown to respond also to indicators of social threat, specifically in nearby space (de Borst et al. 2020; Ellena et al. 2021). A threatening character invading one's personal space is associated with increased activity in ventral premotor cortex and intraparietal sulcus (areas that are part of the brain network coding PPS) as well as amygdala and anterior insula (de Borst and de Gelder 2022). Another line of research using electroencephalography (EEG) has shown that threatening body expression impact early event-related potentials (ERPs), such as N170 and vertex positive potential (VPP) (Stekelenburg and de Gelder 2004; Van Heijnsbergen et al. 2007). These electrophysiological measures of threat also interact with

Received: February 24, 2023. **Revised:** April 11, 2023. **Accepted:** April 12, 2023

PPS. A behavioral ERP study used a modified version of a paper-and-pencil validated measure of comfortable interpersonal distance (CID) to explore how participants react to the threat of interpersonal distance invasion (Perry et al. 2013). Participants were instructed to imagine they were in the center of the room, and as a friend or stranger approached, they could press a key to show that they wanted to stop the person from coming closer. It was observed that the potential threat (approaching person) elicited larger N1 for strangers compared to friends, whereas friends/strangers had no significant effect on P1 and LPP components. These ERP responses occurred from 50 to 800 ms. Besides distance, another critical factor for adaptive threat response is related to control over the threat. Threat experience may be reduced when, for example, threat escape or another behavioral control is possible (Terburg et al. 2018). Active control behavior refers to a sense of control that can reduce or stop the approaching threat (Iachini et al. 2016; Wendt et al. 2017).

A major obstacle in research on human behavior in the face of social threat is the difficulty of rendering threatening situations in a realistic manner and obtaining valid measures of human behavior and physiology. The use of virtual reality (VR) opens unique chances for this important research field (Parsons et al. 2017; Monti and Aglioti 2018) as it allows participants to experience a threatening event in a controlled laboratory environment "as if" it was actually happening to them (Fusaro et al. 2016; Tieri et al. 2017; de Borst et al. 2020; de Borst and de Gelder 2022; Mello et al. 2022). VR-based designs implementing social threat from avatars have successfully been used in behavioral, fMRI and EEG studies (Stolz et al. 2019; de Borst and de Gelder 2022; Mello et al. 2022). Here, we combined VR with behavioral measures and measures of neural and cardiac activity to assess with millisecond temporal resolution the impact of the avatar emotion (angry/neutral) and various levels of threat-control success (0, 25, 50, 75, or 100%). Our goal was to measure how social threat is perceived under naturalistic conditions implemented in VR and whether the ability to effectively control the threat affects how the source of the threat is processed at behavioral, neural, and cardiac levels.

Methods

Participants

Thirty healthy right-handed participants were recruited for this study. All participants had normal or corrected-to-normal vision without brain injury, history of psychiatric disorder, or current psychotropic medication. Participants provided written consent at the beginning of the experiment. They earned 7.5EUR or received one credit point per hour of participation. Four participants' data were rejected because they did not press a button in more than 50% of the trials. Twenty-six participants' data were included in the analysis (13 females, 13 males; age range 18–29 years, mean = 24.65; standard deviation (SD) = 3.60). The Ethical Committee of Maastricht University approved the study, and all procedures conformed to the Declaration of Helsinki.

Design and procedures

VR scenario

The VR scenario consisted of a dark and narrow urban street, in which an avatar expressing an angry or neutral emotion, appeared and subsequently approached the participant. The VR scenario was programmed in Unity 3D (Unity Technologies, US). The basic design of the angry (raised arms) and neutral (arms down) body expressions were similar to a previous study (Mello et al. 2022), while the VR environment and the task settings were new for the present study. Before EEG data collection started, participants put on the VR headset (HTC VIVE) and freely explored the 3D VR world by physically moving their head and walking in the lab. This allowed them to walk along streets in the VR scenario and visually explore the surroundings. This served to make participants immersed in the VR environment.

Experimental design

The VR environment and task were explained to the participants. Participants were told that an angry or emotionally neutral avatar would appear in a dark, urban environment and approach them. They were informed that pressing a control button (space bar) could stop the avatar from coming closer, and they were encouraged to do so as soon as they felt uncomfortable. At the beginning of each trial, a cue appeared indicating the likelihood that pressing the space bar would effectively stop the avatar. There were five different controllable cue conditions (Fig. 1A). In the 0% condition, the button press never stopped the approaching avatar, while in the 100% condition pressing the space bar always stopped the avatar. In the intermediate conditions, the bar press stopped the avatar from approaching with 25, 50, and 75% probability. A sketch of a trial is shown in Fig. 1B. All trials were preceded by a cue presented 1 s before the avatar's appearance. After a 1 ± 0.1 s interval, the avatar was first standing still for 1 ± 0.1 s at a virtual distance from the participant of 5 m. The avatar then started moving towards the participant at a speed of 1.43 m/s. The trial procedure in Fig. 1B shows two screenshots corresponding to the participants' view during the VR experiment. The first screenshot (left) shows the static avatar and the second screenshot (right) shows the approaching avatar. The approach of the avatar was simulated by increasing the size of the avatar over time, covering an increasing portion of the participants' field of view (videos of the approaching avatar can be found in the Supplementary material 1). Participants were instructed to press the button as soon as they felt uncomfortable after the avatar approaching. In some trials, the avatar stopped as participants pressed the button, while at other trials (those with control success $< 100\%$), the button press did not always stop the avatar from approaching. If participants stopped the avatar successfully, the avatar remained still at its position until the next trial. The duration from the advent of the avatar until its disappearance was 3.5 s.

The study used a 5×2 within-subject design with five controllable cue conditions and two avatar emotions (angry, neutral) conditions. There were 40 trials per condition, and the total number of 400 trials was presented randomly in five runs, lasting in total 1 h.

EEG acquisition

EEG data were recorded using an international 10–20 system, a scalp cap with 63 electrodes, and a sampling frequency of 250 Hz (BrainVison Products, Munich, Germany). The electrode positioned on Cz was used as the reference during recording, and the forehead electrode positioned on FP1 was used as a ground electrode. Four electrodes were used to measure the electrooculogram (EOG). Two of them were used as vertical electrooculograms (VEOG). One was placed above the right eye, and another was placed below the right eye. The other two electrodes were used as a horizontal electrooculogram (HEOG), with one placed at the outer canthus of the left eye, and the other at the outer canthus of the right eye. Three electrodes were used for electrocardiography (ECG). Two ECG electrodes were put one centimeter below the center of the left and right collarbones separately. The third ECG electrode was put on the right waist. The remaining 56 electrodes covered the whole scalp, including locations FPz, AFz, Fz, FCz, CPz, Pz, POz, Oz, AF7, AF8, AF3, AF4, F7, F8, F5, F6, F3, F4, F1, F2, FC5,

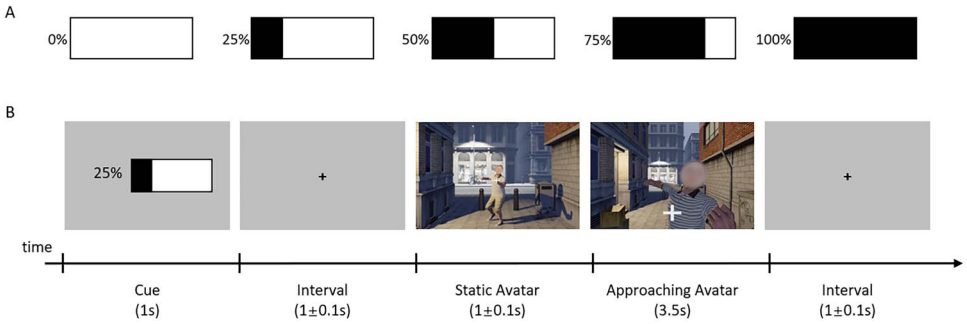

Fig. 1. (A) Five kinds of controllable cues. (B) A trial procedure.

Fig. 2. VR-chin rest-EEG setup shows a participant standing against the height-adjustable bar chair.

FC6, FC3, FC4, FC1, FC2, T7, T8, C5, C6, C3, C4, C1, C2, TP7, TP8, CP5, CP6, CP3, CP4, CP1, CP2, P7, P8, P5, P6, P3, P4, P1, P2, PO7, PO8, PO3, PO4, O1, and O2. Impedances for reference and ground were maintained below 5 kOhm and all other electrodes below 10 kOhm. After lowering impedance, the VR headset was carefully placed on the chin rest. The participants were standing against a height-adjustable bar chair in front of a high desk with the VR headset-Chin rest setup (Fig. 2).

The heavy VR headset could potentially influence the EEG signal and cause head movement during the EEG data collection. To reduce these risks, we combined VR with a chin rest in our EEG experiment. The reason for this choice was that EEG is highly sensitive to stimulus phase-locked neural activity and muscle activity. More specifically, we focused the analysis on ERPs to the static avatar instead of the dynamic avatar because of the higher difficulty of obtaining clean and stable ERPs to dynamic stimuli. We refrained from investigating movements in the VR environment because it would have induced large motor-related activity. While this would have further added to the external validity of the study, it would have confounded the ERPs to the emotional stimuli that were the focus of the study. Therefore, we think that limiting the investigation to static 3D representations helped us to obtain cleaner and more reliable neural measures of emotional processing, which we considered as most important.

EEG data preprocessing

EEG data were preprocessed and analyzed using FieldTrip version 20,220,104 (Oostenveld et al. 2011) in Matlab R2021b (MathWorks, U.S.). The signal was first segmented into epochs from 1,000 ms pre-stimulus (the static avatar) to 2,000 ms post-stimulus and then filtered with a 0.1–30-Hz band-pass filter. EEG data at each electrode were re-referenced to the average of all electrodes. Artifact rejection was done using independent component analysis (ICA, logistic infomax ICA algorithm; Bell and Sejnowski 1995); on average, 1.88 ± 0.33 (mean $\pm$ SD) components were removed per participant. Finally, single trials during which the peak amplitude exceeded 3 SD above/below the mean amplitude were rejected. On average, $75.36 \pm 5.27\%$ (mean $\pm$ SD) trials were preserved and statistically analyzed per participant.

Event-related potential analyses

The ERP analyses performed were time locked to the presentation of the static avatar to derive clean ERPs in response to the still image. Here, a time window from 200 ms before the onset of static avatar until 1,000 ms after the onset was extracted from each trial of the preprocessed data. A baseline correction was applied by subtracting the average amplitude during the interval ($-200 \sim 0$ ms) before the onset of the static avatar. The segmented EEG for each participant was averaged for each experimental condition, resulting in ERPs used for further statistical analyses, which were performed using IBM SPSS Statistics 27 (IBM Corp., Armonk, NY, USA). In the ERP analysis, we focused on the ERPs elicited by social threatening/non-threatening body expressions (as represented by angry/neutral avatars) and their sensitivity to the level of threat control (controllable cues). We separated the EEG channels into five spatial clusters and identified for each region a prominent ERP component and centered a time window on its peak based on visual inspection of the overall ERP waveform, topographical distribution of grand-averaged ERP and previous studies (de Gelder et al. 2004; Stekelenburg and de Gelder 2004; Cunningham et al. 2005; Van Heijnsbergen et al. 2007; Luo et al. 2010; He et al. 2011; Chai et al. 2022). The resulting ERP components and associated time windows are shown for each region in Table 1. The mean amplitude was computed as the average of all electrodes within the cluster within the specific time window.

A repeated-measures 5×2 ANOVA (Controllable cue: 0%/25%/50%/75%/100% $\times$ Avatar emotion: angry/neutral) was applied to the mean amplitudes; this was done for each ERP component separately. Degrees of freedom for F-ratios were corrected with the Greenhouse–Geisser method. Statistical differences were considered as significant given a $P < 0.05$. To control for type I errors, a Bonferroni correction was applied to the P-values associated with the main effects and interaction effects of every ERP component. Only corrected P-values were reported.

Time-frequency analyses

To assess temporal variations in oscillatory EEG power within the range from 1 to 30 Hz, we decomposed each trial using the complex Morlet wavelet transform (frequency-bin size: 1 Hz, three cycles per time window, time-bin size: 50 ms). To reduce edge effects, we applied the time-frequency analysis to epochs

Table 1. Brain regions and electrodes of ERP components and associated time windows.

ERPs	Brain regions	Electrodes	Time windows
N170	Temporal	P7, P8, TP7, TP8, CP5, CP6, P5, P6	180–230 ms
VPP	Central-occipital midline	Cz, CPz, Pz, POz, Oz	200–250 ms
P3	Parietal	P5, P6, P7, P8, PO7, PO8	280–350 ms
N3	Frontal-central (with midline)	FCz, Cz, FC1, FC2, C1, C2	300–350 ms
LPP	Frontal-central (without midline)	FC5, FC6, F5, F6, F7, F8, C5, C6	500–800 ms

of longer duration (corresponding to the duration of the pre-processed epochs before ERP computation; see above) and used a longer and earlier baseline in the interval (−500 ∼ −100 ms) before the onset of the static avatar. We focused the statistical analysis on oscillatory power in the theta (4–7 Hz) band, based on literature showing that theta activity is related to the processing of threat and control, especially at frontal and central scalp regions (DeLaRosa et al. 2014; Ma et al. 2016; Lange et al. 2022). Thus, electrodes positioned at Fz, FCz, Cz, F1, F2, FC1, FC2, C1, and C2 were selected for this analysis. Inspection of theta power revealed a peak between 100 and 200 ms after the onset time in the frontal central region consistently across conditions. Based on this observation, we extracted mean theta power during the time window (100–200 ms) at the selected electrodes and statistically analyzed it using the same repeated measures ANOVAs as for the ERP analysis; see above.

ECG analyses

A time window from 500 ms before static avatar onset to 4,500 ms after the onset was extracted from the continuous ECG data. The ECGdeli toolbox (Pilia et al. 2021) was used for analyzing heart rate. One participant's ECG data were not recorded; thus, 25 participants' ECG data were included in the analysis. The electrode that was placed under the left collarbone was selected for this analysis as it was positioned closest to the heart, giving the strongest signal. Statistical analyses were the same as for ERP and theta power as discussed above.

Behavioral analyses

We instructed participants to press the button as soon as they felt uncomfortable with the approaching avatar. In some trials, participants pressed the button once (4.81% trials), while in other trials, participants did not press the button or pressed it more than once (16.42% trials). Two behavioral indicators were recorded. First, the virtual distance between the participant and avatar at the time when participants first pressed the button. For this, the time at which the participants pressed the response button was multiplied by the speed by which the avatar was approaching and this was subsequently subtracted by the distance at which the avatar initially appeared (distance = 3.5-response time × speed). Second, the number of button presses was recorded. Like the physiological measures above, each behavioral indicator was subjected to a 5 (controllable cue: 0%/25%/50%/75%/100%) × 2 (Avatar emotion: angry/neutral) repeated-measures ANOVA.

VR questionnaire

Information about the participants' subjective experience during the VR scenario was obtained with a questionnaire, which participants filled in after the experiment (Seinfeld et al. 2016; Seinfeld et al. 2021). The individual questionnaire items are shown in Table 2.

Results

VR questionnaire results

The items of the VR questionnaire and the mean ± SD of each item scores are shown in Table 2. We used a 7-point scale to test subjective feelings during the experiment, taking the median value "4" (the neutral subjective experience) as a reference to which we compared participants' scores on each item. One-sample *t*-test results showed that realism (t (25) =2.74, $P = 0.011$), attention to cue (t (25) = 3.61, $P = 0.001$), fear of approaching angry avatar (t (25) = 4.55, $P < 0.001$) and fear of approaching neutral avatar (t (25) = 2.46, $P < 0.021$) were significantly larger than the reference value of 4, while fear of possible assault (t (25) = −2.33, $P = 0.028$), fear of static angry avatar (t (25) = −2.36, $P = 0.026$), and fear of static neutral avatar (t (25) = −7.75, $P < 0.001$) were significantly smaller than the reference value. Furthermore, subjective experience of vulnerability (t (25) = −1.12, $P = 0.904$) and violence (t (25) = −1.14, $P = 0.266$) were not significant. Paired t-test results revealed that fear of a static angry avatar was significantly larger than fear of a static neutral avatar (t (25) = 4.44, $P < 0.001$), and fear of an approaching angry avatar was significantly larger than fear of an approaching neutral avatar (t (25) = 3.99, $P < 0.001$).

Behavioral results

For the first behavioral indicator (distance), the main effect of emotion was significant (F (1, 25) = 14.33, $P < 0.001$, $\eta_p^2 = 0.36$) such that the distance between participants and the avatar was bigger when they saw the angry (2.24 ± 0.23) than neutral avatar (1.82 ± 0.21). The main effect of controllable cue was significant too (F (4, 100) = 4.56, $P = 0.029$, $\eta_p^2 = 0.15$). A paired *t*-test between each controllable cue condition revealed no significant results after Bonferroni correction. The linear effect of controllable cue was significant (F (1, 25) = 5.07, $P = 0.033$, $\eta_p^2 = 0.17$), showing that as the probability of the controllable cue increased, the tolerated distance decreased. The interaction effect between emotion and controllable cue was non-significant (F (4, 100) = 2.28, $P = 0.096$, $\eta_p^2 = 0.08$) (Fig. 3A).

Applying the same analyses to the second behavioral indicator (number of button presses) yielded qualitatively identical results, showing more button responses to the angry vs neutral avatar and to low vs. high probabilities of control success (main effect of avatar emotion: F (1, 25) = 4.43, $P = 0.045$, $\eta_p^2 = 0.15$, angry: 1.61 ± 0.25, neutral avatar: 1.40 ± 0.18; main effect of controllable cue: (F (4, 100) = 6.15, $P = 0.016$, $\eta_p^2 = 0.20$); linear effect of the controllable cue: F (1, 25) = 6.58, $P = 0.017$, $\eta_p^2 = 0.21$; interaction effect (not significant): F (4, 100) = 1.83, $P = 0.178$, $\eta_p^2 = 0.07$) (Fig. 3B).

ERPs

N170

The main effect of avatar emotion on the N170 amplitude was significant (F (1, 25) = 9.77, $P = 0.017$, $\eta_p^2 = 0.28$) such that the angry avatar elicited larger N170 amplitudes (−2.04 ± 0.48 μV) than the

Table 2. The items and mean ± SD rating scores in the VR questionnaire are shown. Ratings were made on a 7-point scale (1 = not at all, 7 = completely).

Item	Question	Mean ± SD
Realism	To what extent have you experienced the situation as if it was real?	4.69 ± 1.29
Vulnerable	Did you feel at any time that you were vulnerable?	3.96 ± 1.61
Violent	How violent do you find this scene is?	3.69 ± 1.38
Assaulted	Did you think that you could be physically assaulted during the scene?	3.19 ± 1.77
Attention to cue	How much attention did you pay to the probability cues during the experience?	5.08 ± 1.52
Fear of static angry avatar	How fearful did you feel when facing the static angry avatar?	3.23 ± 1.67
Fear of an approaching angry avatar	The sense of uncomfortable increased when the avatar got closer to me.	5.38 ± 1.55
Fear of static neutral avatar	How fearful did you feel when facing the static neutral avatar?	1.96 ± 1.34
Fear of an approaching neutral avatar	The sense of uncomfortable increased when the avatar got closer to me.	4.69 ± 1.44

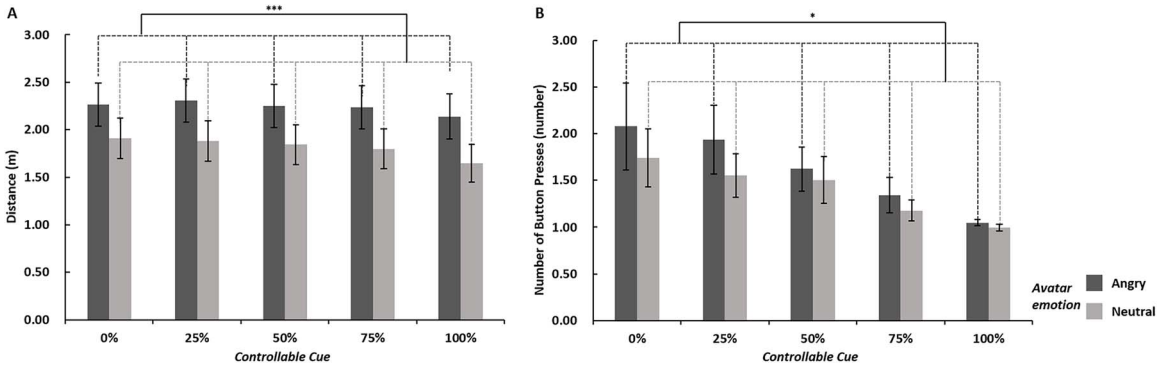

Fig. 3. (A) Means and SE of distance per condition. (B) Means and SE of the number of button presses per condition. ***$P < 0.001$, *: $P < 0.05$.

neutral avatar (−1.68 ± 0.44 μV). The main effect of controllable cue (F (4, 100) = 0.34, $P = 1$, $\eta_p^2 = 0.01$) and the interaction of the two factors were not significant (F (4, 100) = 1.23, $P = 1$, $\eta_p^2 = 0.05$) (Fig. 4).

VPP

The main effect of avatar emotion on VPP was significant (F (1, 25) = 12.63, $P = 0.006$, $\eta_p^2 = 0.34$) such that the angry avatar elicited larger VPP amplitudes (3.50 ± 0.53 μV) than the neutral avatar (2.93 ± 0.51 μV). The main effect of the controllable cue (F (4, 100) = 1.06, $P = 1$, $\eta_p^2 = 0.04$) and the interaction of the two factors were not significant (F (4, 100) = 0.12, $P = 1$, $\eta_p^2 = 0.01$) (Fig. 5).

N3

The main effect of avatar emotion on N3 was significant (F (1, 25) = 9.28, $P = 0.021$, $\eta_p^2 = 0.27$), such that the angry avatar elicited smaller amplitudes (−1.83 ± 0.25 μV) than the neutral (−2.12 ± 0.26 μV) avatar. The main effect of the controllable cue (F (4, 100) = 2.37, $P = 0.300$, $\eta_p^2 = 0.09$) and the interaction of the two factors were not significant (F (4, 100) = 0.99, $P = 1$, $\eta_p^2 = 0.04$) (Fig. 6).

P3

The main effect of avatar emotion on P3 was not significant (F (1, 25) = 4.81, $P = 0.150$, $\eta_p^2 = 0.16$). The main effect of controllable cue (F (4, 100) = 1.36, $P = 1$, $\eta_p^2 = 0.05$) and the interaction of the two factors were not significant (F (4, 100) = 0.33, $P = 1$, $\eta_p^2 = 0.01$).

LPP

The main effect of controllable cue on LPP was significant (F (4, 100) = 4.24, $P = 0.034$, $\eta_p^2 = 0.15$), such that the 100% cue elicited larger amplitudes (0.18 ± 0.25 μV) than the 75% cue (−2.56 ± 0.26 μV). The main effect of avatar emotion was not significant (F (1, 25) = 1.47, $P = 0.950$, $\eta_p^2 = 0.05$). The interaction of controllable cue and avatar emotion was not significant (F (4, 100) = 2.68, $P = 0.171$, $\eta_p^2 = 0.10$). (Fig. 7).

Time-frequency results

The main effect of avatar emotion on frontocentral theta power was significant (F (1, 25) = 7.87, $P = 0.010$, $\eta_p^2 = 0.24$): theta power under the angry avatar condition (159.48 ± 20.68 dB) was increased compared to neutral avatar condition (140.24 ± 20.85 dB). The main effect of controllable cue (F (4, 100) = 0.84, $P = 0.501$, $\eta_p^2 = 0.03$) and the interaction of the two factors were not significant (F (4, 100) = 0.74, $P = 0.544$, $\eta_p^2 = 0.03$) (Fig. 8).

ECG results

Avatar emotion had a significant main effect on ECG (F (1, 24) = 7.482, $P = 0.012$, $\eta_p^2 = 0.24$) such that the angry avatar elicited a higher heart rate (77.84 ± 2.49 beats per minute, BPM) than the neutral avatar (77.55 ± 2.45 BPM) did. The main effect of controllable cue (F (4, 96) = 1.24, $P = 0.301$, $\eta_p^2 = 0.05$) and the interaction of the two factors were not significant (F (4, 96) = 0.45, $P = 0.744$, $\eta_p^2 = 0.02$) (Fig. 9).

Discussion

In this study, we investigated the behavioral, EEG, and cardiac responses of human participants that were facing angry and neutral avatars in a VR environment in which they had control various degrees of control over the interaction with the avatar. Behaviorally, we observed a difference in the time/distance at which participants felt uncomfortable with the approaching avatar depending on the presence of threat. This is in line with the

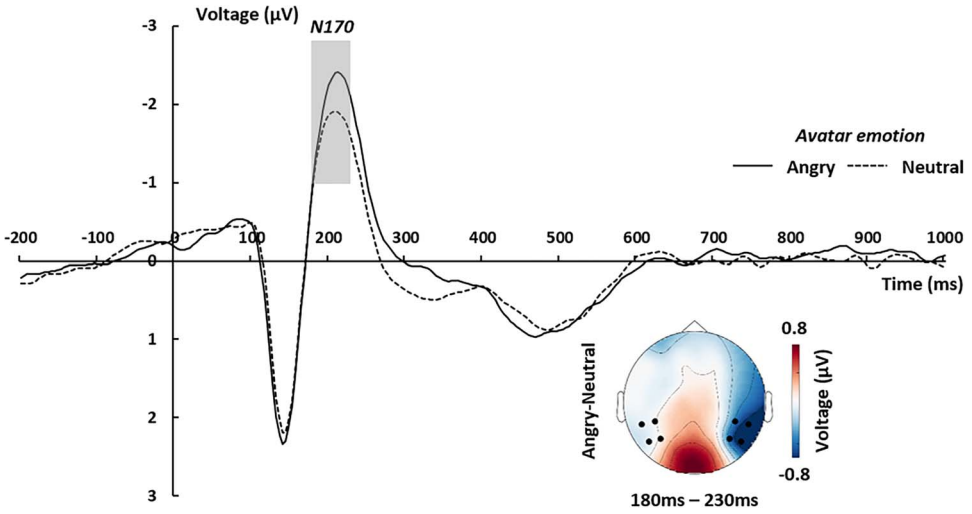

Fig. 4. Grand-averaged ERP waveforms of N170 per avatar emotion condition. Waveforms were calculated by averaging the data at the electrodes P7, P8, TP7, TP8, CP5, CP6, P5, and P6, and across the controllable cue conditions. The "angry" minus "neutral" topographic map was calculated by averaging the data within a time window of 180–230 ms after the onset of the static avatar. The black dots highlight the electrodes that were used to calculate grand-averaged ERPs.

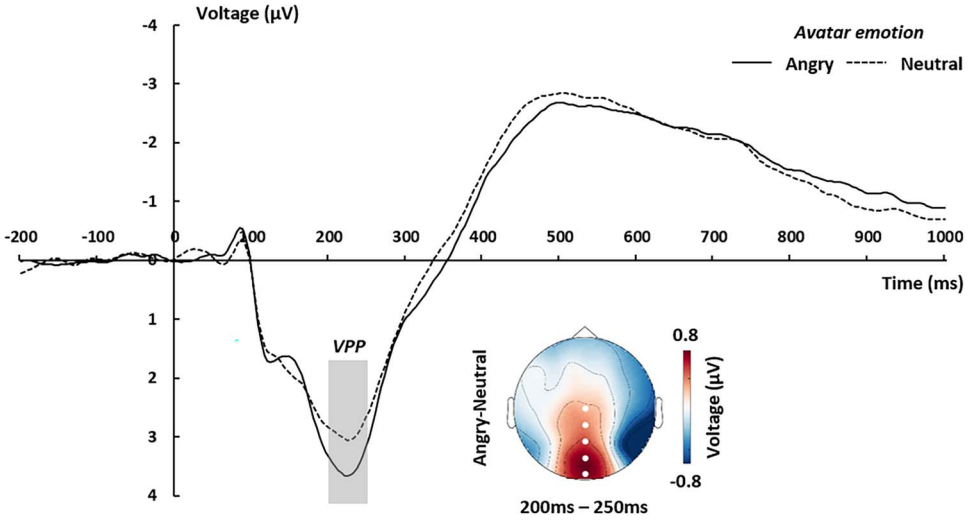

Fig. 5. Grand-averaged ERP waveforms of VPP per avatar emotion condition. Waveforms were calculated by averaging the data at the electrodes Cz, CPz, Pz, POz, and Oz, and averaged across controllable cue conditions. The "angry" minus "neutral" topographic map was calculated by averaging the data within a time window of 200–250 ms after the onset of the static avatar. The white dots highlight the electrodes that were used to calculate grand-averaged ERPs.

literature showing that threat imminence triggers defensive behavior (Blanchard and Blanchard 1990; de Haan et al. 2016; Qi et al. 2018; Terburg et al. 2018; Riem et al. 2019). The impact of personal distance for social threat experience was first shown with full body expression of avatars in a study using VR and fMRI (de Borst et al. 2020). Combining VR with EEG in the present study now allows a detailed picture of the time courses. The questionnaire results also suggested that participants felt more threatened when facing an angry than a neutral avatar. Concerning the impact of controllability, we found a significant effect of the controllable cue condition for each of the two behavioral indicators. First, as the probability of successful control increased, the distance from the avatar that participants judged tolerable decreased. This result is supported by a previous behavioral study (Iachini et al. 2016). Second, we observed that as the probability of successful control decreased, the number of button presses increased. This is consistent with the notion that the closer a threatening stimulus is to the self, the more likely the danger and the stronger the elicited defensive responses (Bufacchi 2017). In our experiment, the button press was regarded as a defensive behavior. As the chances of successfully stopping the approaching avatar became higher, the number of button presses (defensive behavior) decreased.

At the neural level, we have three major findings. Seeing a threatening body expression (angry avatar) increased the amplitude of early ERP components (N170 and VPP) compared to non-threatening body expressions (neutral avatar). Furthermore, threatening body expressions elicited a smaller N3 than neutral body expressions. Finally, full control (100% controllable cue) increased the amplitude of the late component LPP as compared to the 75% controllable cue. Taken together, we show that social threat is detected in the early stages and independently of the possibility of control. In contrast, the impact of perceived control

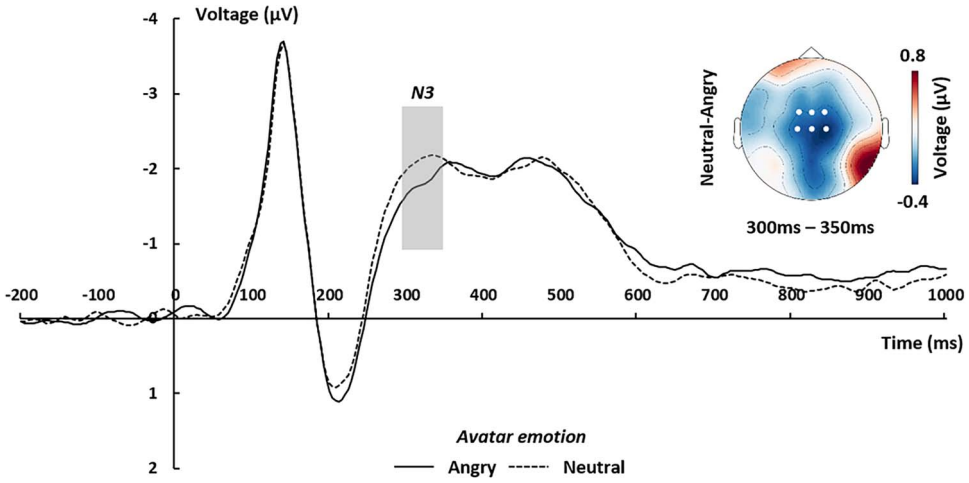

Fig. 6. Grand-averaged ERP waveforms of frontal-central N3 per avatar emotion condition. Waveforms were calculated by averaging the data at the electrodes FCz, Cz, FC1, FC2, C1, and C2, and averaged across controllable cue conditions. The "neutral" minus "angry" topographic map was calculated by averaging the data within a time window of 300–350 ms after the onset of the static avatar. The white dots highlight the electrodes, which were used to calculate grand-averaged ERPs.

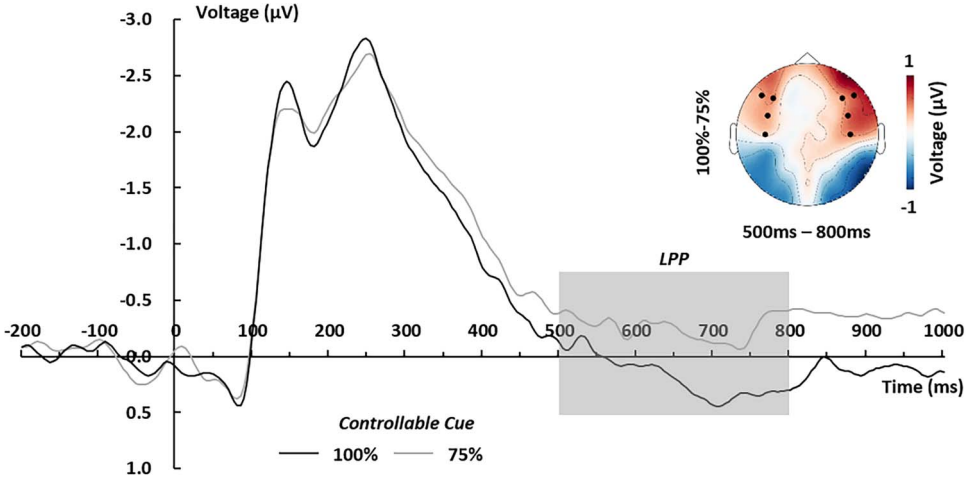

Fig. 7. Grand-averaged ERP waveforms of frontal-center LPP under the 100 and 75% controllable cue conditions. Waveforms were calculated by averaging the data at the electrodes FC5, FC6, F5, F6, F7, F8, C5, and C6. The 100% controllable cue condition minus 75% controllable cue condition topographic map was calculated by averaging the data within a time window of 500–800 ms after the onset of the static avatar. The black dots are highlighted electrodes, which were used to calculate grand-averaged ERPs.

over the threat is reflected in the electrophysiological responses at later stages.

Early threat detection. Our results indicate that participants were more sensitive to affective stimuli than neutral ones in the early stages of full body avatar processing. There are consistent but relatively few findings on body perception, a situation reflecting that whole body perception is still much less studied than face perception. Previous studies have reported that not only facial expressions but also whole body images trigger this early brain activity (Stekelenburg and de Gelder 2004; Meeren et al. 2005; Van Heijnsbergen et al. 2007; Farzmahdi et al. 2021) and that the activity in this time window is sensitive to the emotional expression as shown by larger VPP amplitudes for a fearful than a neutral body (Stekelenburg and de Gelder 2004). Also, consistent with our results, N170 and VPP seem to derive from a common source in the brain (Joyce and Rossion 2005). An interesting finding consistent with the present results is that presenting a target stimulus preceding the body stimulus did not influence the N170 amplitudes to the body stimulus (Hietanen et al. 2014), indicating that body expression perception is an automatic-stimulus-driven process. Here, we add to this by showing that clear knowledge of subjective control of the threat does not impact the course of early body expression perception. This result suggests that we are observing here the early stages of threat perception, which are then followed by calculations of alternative escape decisions (Qi et al. 2018). Given this interpretation of the processes associated with N170, it is worth stressing that our results were obtained in a VR setting, which is characterized by an immersive experience of realism but also at the same time, a subjective understanding that the experience is not real, in our case that the participant is not really threatened. An alternative outcome might have been that participants knowledge of the danger being "unreal" would have overruled this early signature of threat experience.

Temporal dynamics of behavioral control. The middle-late component N3 is related to source allocation and response preparation. A lower amplitude of the N3 component is thought to reflect that more cognitive resources and brain resources are being mobilized to prepare for a response to the threat (Coenen 1995; Mayer et al. 2021; Ke et al. 2022); e.g. higher cognitive tasks have been shown to elicit lower N3 amplitudes than simpler tasks (Michida et al. 1998).

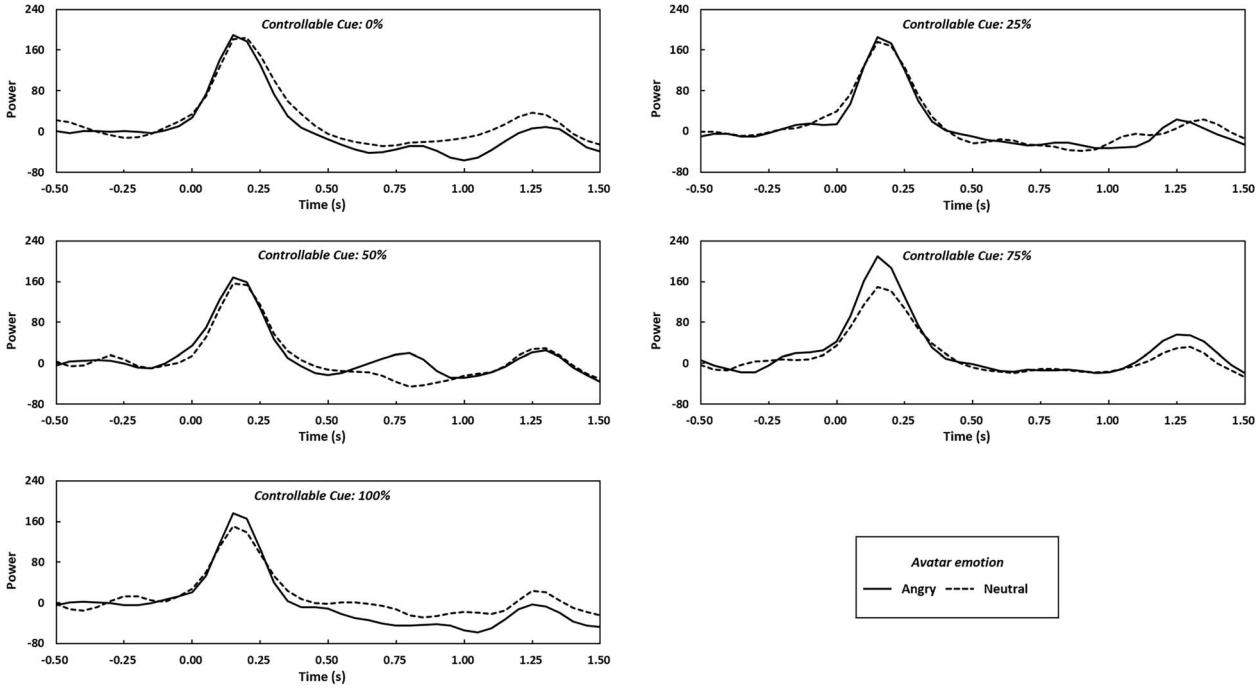

Fig. 8. Theta power was calculated by averaging the theta band (4–7 Hz) at the electrodes Fz, FCz, Cz, F1, F2, FC1, FC2, C1, and C2 per condition.

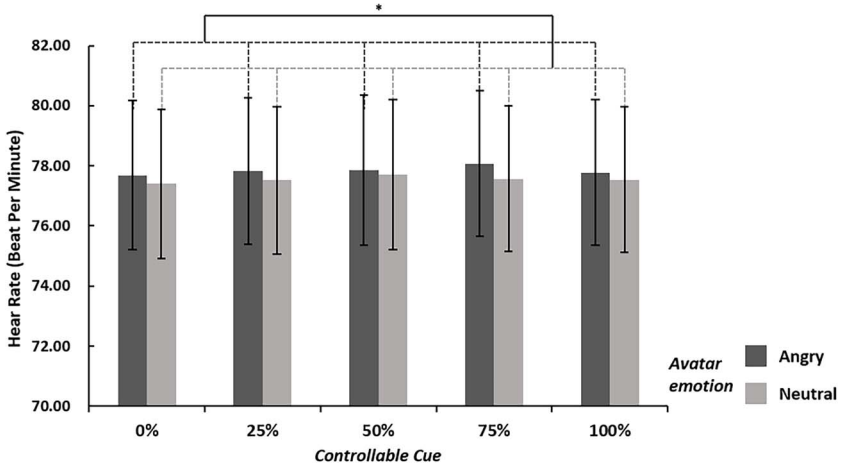

Fig. 9. Means and SE of heart rate per condition. *$P < 0.05$.

Moreover, negative emotional visual stimuli have been observed to evoke lower N3 than positive emotional ones (Ke et al. 2022). In our experiment, we found threatening body expressions to elicit lower N3 than neutral body expressions, suggesting that the threatening stimuli elicited negative emotions and required more cognitive resources than the neutral stimuli.

Concerning the late positive potential (LPP), previous studies reported that LPP refers to task-relevant, motivational engagement and action preparation during the later stage (Gable et al. 2015; Di Lemma et al. 2020; Gantiva et al. 2020). Johnen and Harrison found that LPP amplitude was larger under conditions of certainty compared to less certain conditions (Johnen and Harrison 2020). In line with this study, we found that perfect control (100% controllable cue) elicited larger LPP than the 75% controllable cue. This suggests that perfect control opportunity resulted in more motivation engagement than 75% control success.

We also examined oscillatory brain responses in relation to differences in successful control probability for threatening and neutral body expression. Our data show that theta power in frontal central regions was only modulated by avatar emotion. There was a significant increase in response to the threatening body expression (angry avatar) compared with the neutral body expression (neutral avatar). This is consistent with findings showing that increased theta power is related to higher emotional arousal (Aftanas et al. 2001; Aftanas et al. 2002; Sulpizio et al. 2021) and that greater theta power may be induced by social threat compared with non-threat stimuli (Diao et al. 2017).

Our ECG results are consistent with the literature showing a higher heart rate for social threat than for non-threat (Weeks and Zoccola 2015; Eisenbarth et al. 2016), although another study found a lower heart rate for threatening vs neutral body expressions (Mello et al. 2022). In that study, participants passively viewed a threatening avatar coming closer, which induced the freezing response reflected in a reduced heart rate. In our paradigm, participants could actively stop the approaching avatar from coming closer by pressing the button. Thus, the increased

heart rate might reflect emotional arousal to the threatening body expression rather than a freezing response.

In conclusion, the amplitudes of the earlier components (N170/VPP/N3) are elicited by viewing a threatening body expression and seem to be independent of control opportunities, while the latter modulate the later LPP component. Our findings on N170/VPP effects show that these two components may be modulated by threatening/neutral body expressions, which may reflect mechanisms involved in rapid detection of social threat in an early-middle stage, such as decoding the meaning of a threatening body expression. The social threat is further processed in later stages, as indicated by the effects of avatar emotion on the middle-late cognitive components N3. The ability to control the threat shows in the late cognitive evaluation stages, as reflected by the LPP effects. In addition, the increased frontal central theta power and heart rate are related to social threat processing. In sum, our study provides behavioral and neural insights into how humans process social threats under varying levels of control. On the methodological side, our study presents a novel VR-EEG-ECG setup that will be useful also for future VR and EEG studies investigating social interaction situations in a naturalistic fashion.

Author contributions

Juanzhi Lu (Conceptualization, Data curation, Formal analysis, Investigation, Methodology, Validation, Visualization, Writing—original draft, Writing—review & editing), Selma Kemmerer (Conceptualization, Formal analysis, Investigation, Writing—review & editing), Lars Riecke (Formal analysis, Writing—review & editing), Beatrice de Gelder (Conceptualization, Funding acquisition, Project administration, Supervision, Writing—original draft, Writing—review & editing).

Supplementary material

Supplementary material is available at *Cerebral Cortex* online.

Funding

This work was supported by the European Research Council (ERC) FP7-IDEAS-ERC (Grant agreement number 295673; Emobodies), by the ERC Synergy grant (Grant agreement 856495; Relevance), by the Future and Emerging Technologies (FET) Proactive Program H2020-EU.1.2.2 (Grant agreement 824160; EnTimeMent), by the Industrial Leadership Program H2020-EU.1.2.2 (Grant agreement 825079; MindSpaces), by the Horizon 2020 Programme H2020-FETPROACT-2020-2 (grant 101017884 GuestXR) and by China Scholarship Council (CSC202008440538).

Conflict of interest statement: The authors declare that no conflict of interest exists.

References

Aftanas L, Varlamov A, Pavlov S, Makhnev V, Reva N. Affective picture processing: event-related synchronization within individually defined human theta band is modulated by valence dimension. *Neurosci Lett*. 2001:303(2):115–118.

Aftanas LI, Varlamov AA, Pavlov SV, Makhnev VP, Reva NV. Time-dependent cortical asymmetries induced by emotional arousal: EEG analysis of event-related synchronization and desynchronization in individually defined frequency bands. *Int J Psychophysiol*. 2002:44:67–82.

Avenanti A, Annela L, Serino A. Suppression of premotor cortex disrupts motor coding of peripersonal space. *NeuroImage*. 2012:63(1):281–288.

Bell AJ, Sejnowski TJ. An information-maximization approach to blind separation and blind deconvolution. *Neural Comput*. 1995:7:1129–1159.

Blanchard RJ, Blanchard DC. An ethoexperimental analysis of defense, fear, and anxiety. In: McNaughton IN, Andrews G, editors. *Anxiety*. University of Otago Press, Dunedin (NZ); 1990. pp. 124–133.

Blanchard RJ, Flannelly KJ, Blanchard DC. Defensive behaviors of laboratory and wild *Rattus norvegicus*. *J Comp Psychol*. 1986:100:101.

Bogdanova OV, Bogdanov VB, Dureux A, Farnè A, Hadj-Bouziane F. The peripersonal space in a social world. *Cortex*. 2021:142:28–46.

de Borst AW, de Gelder B. Threat detection in nearby space mobilizes human ventral premotor cortex, intraparietal sulcus, and amygdala. *Brain Sciences*. 2022:12(3):391.

de Borst AW, Sanchez-Vives MV, Slater M, de Gelder B. First-person virtual embodiment modulates the cortical network that encodes the bodily self and its surrounding space during the experience of domestic violence. *eNeuro*. 2020:7(3):ENEURO.0263–ENEU19.2019.

Brozzoli C, Gentile G, Bergouignan L, Ehrsson HH. A shared representation of the space near oneself and others in the human premotor cortex. *Curr Biol*. 2013:23(18):1764–1768.

Bufacchi RJ. Approaching threatening stimuli cause an expansion of defensive peripersonal space. *J Neurophysiol*. 2017:118(4):1927–1930.

Bufacchi RJ, Iannetti GD. An action field theory of peripersonal space. *Trends Cogn Sci*. 2018:22(12):1076–1090.

Chai X, Liu M, Huang T, Wu M, Li J, Zhao X, Yan T, Song Y, Zhang YX. Neurophysiological evidence for goal-oriented modulation of speech perception. *Cereb Cortex*. 2022:33(7):3910–3921.

Cléry J, Guipponi O, Wardak C, Hamed SB. Neuronal bases of peripersonal and extrapersonal spaces, their plasticity and their dynamics: knowns and unknowns. *Neuropsychologia*. 2015:70:313–326.

Coenen AM. Neuronal activities underlying the electroencephalogram and evoked potentials of sleeping and waking: implications for information processing. *Neurosci Biobehav Rev*. 1995:19(3):447–463.

Cunningham WA, Espinet SD, DeYoung CG, Zelazo PD. Attitudes to the right-and left: frontal ERP asymmetries associated with stimulus valence and processing goals. *NeuroImage*. 2005:28(4):827–834.

de Gelder B, Snyder J, Greve D, Gerard G, Hadjikhani N. Fear fosters flight: a mechanism for fear contagion when perceiving emotion expressed by a whole body. *Proc Natl Acad Sci*. 2004:101(47):16701–16706.

de Gelder B, Van den Stock J, Meeren HK, Sinke CB, Kret ME, Tamietto M. Standing up for the body. Recent progress in uncovering the networks involved in the perception of bodies and bodily expressions. *Neurosci Biobehav Rev*. 2010:34(4):513–527.

de Haan AM, Smit M, Van der Stigchel S, Dijkerman HC. Approaching threat modulates visuotactile interactions in peripersonal space. *Exp Brain Res*. 2016:234(7):1875–1884.

DeLaRosa BL, Spence JS, Shakal SK, Motes MA, Calley CS, Calley VI, Hart J Jr, Kraut MA. Electrophysiological spatiotemporal dynamics during implicit visual threat processing. *Brain Cogn*. 2014:91:54–61.

Di Lemma LC, Stancak A, Soto V, Fallon N, Field M. Event-related and readiness potentials when preparing to approach and avoid alcohol cues following cue avoidance training in heavy drinkers. *Psychopharmacology*. 2020:237(5):1343–1358.

Di Pellegrino G, Làdavas E. Peripersonal space in the brain. *Neuropsychologia*. 2015:66:126–133.

Diao L, Qi S, Xu M, Fan L, Yang D. Electroencephalographic theta oscillatory dynamics reveal attentional bias to angry faces. *Neurosci Lett*. 2017:656:31–36.

Eilam D. Die hard: a blend of freezing and fleeing as a dynamic defense—implications for the control of defensive behavior. *Neurosci Biobehav Rev*. 2005:29(8):1181–1191.

Eisenbarth H, Chang LJ, Wager TD. Multivariate brain prediction of heart rate and skin conductance responses to social threat. *J Neurosci*. 2016:36(47):11987–11998.

Ellena G, Starita F, Haggard P, Romei V, Làdavas E. Fearful faces modulate spatial processing in peripersonal space: an ERP study. *Neuropsychologia*. 2021:156:107827.

Farzmahdi A, Fallah F, Rajimehr R, Ebrahimpour R. Task-dependent neural representations of visual object categories. *Eur J Neurosci*. 2021:54(7):6445–6462.

Fusaro M, Tieri G, Aglioti SM. Seeing pain and pleasure on self and others: behavioral and psychophysiological reactivity in immersive virtual reality. *J Neurophysiol*. 2016:116(6):2656–2662.

Gable PA, Adams DL, Proudfit GH. Transient tasks and enduring emotions: the impacts of affective content, task relevance, and picture duration on the sustained late positive potential. *Cognitive, Affective, & Behavioral Neuroscience*. 2015:15(1):45–54.

Gantiva C, Sotaquirá M, Araujo A, Cuervo P. Cortical processing of human and emoji faces: an ERP analysis. *Behav Inform Technol*. 2020:39(8):935–943.

George DT, Ameli R, Koob GF. Periaqueductal gray sheds light on dark areas of psychopathology. *Trends Neurosci*. 2019:42(5):349–360.

Gladwin TE, Hashemi MM, van Ast V, Roelofs K. Ready and waiting: freezing as active action preparation under threat. *Neurosci Lett*. 2016:619:182–188.

Graziano MS, Cooke DF. Parieto-frontal interactions, personal space, and defensive behavior. *Neuropsychologia*. 2006:44(6):845–859.

Hagenaars MA, Roelofs K, Stins JF. Human freezing in response to affective films. *Anxiety, Stress & Coping*. 2014:27(1):27–37.

He WQ, Luo WB, He HM, Chen X, Zhang DJ. N170 effects during exact and approximate calculation tasks: an ERP study. *Neuroreport*. 2011:22(9):437–441.

Hietanen JK, Kirjavainen I, Nummenmaa L. Additive effects of affective arousal and top-down attention on the event-related brain responses to human bodies. *Biol Psychol*. 2014:103:167–175.

Iachini T, Coello Y, Frassinetti F, Senese VP, Galante F, Ruggiero G. Peripersonal and interpersonal space in virtual and real environments: effects of gender and age. *J Environ Psychol*. 2016:45:154–164.

Johnen A-K, Harrison N. Level of uncertainty about the affective nature of a pictorial stimulus influences anticipatory neural processes: an event-related potential (ERP) study. *Neuropsychologia*. 2020:146:107525.

Joyce C, Rossion B. The face-sensitive N170 and VPP components manifest the same brain processes: the effect of reference electrode site. *Clin Neurophysiol*. 2005:116(11):2613–2631.

Ke H, Vuong QC, Geangu E. Three-and six-year-old children are sensitive to natural body expressions of emotion: an event-related potential emotional priming study. *J Exp Child Psychol*. 2022:224:105497.

Lange L, Rommerskirchen L, Osinsky R. Midfrontal theta activity is sensitive to approach–avoidance conflict. *J Neurosci*. 2022:42(41):7799–7808.

LeDoux J, Daw ND. Surviving threats: neural circuit and computational implications of a new taxonomy of defensive behaviour. *Nat Rev Neurosci*. 2018:19(5):269–282.

Livermore JJ, Klaassen FH, Bramson B, Hulsman AM, Meijer SW, Held L, Klumpers F, de Voogd LD, Roelofs K. Approach-avoidance decisions under threat: the role of autonomic psychophysiological states. *Front Neurosci*. 2021:15:621517.

Luo W, Feng W, He W, Wang N-Y, Luo Y-J. Three stages of facial expression processing: ERP study with rapid serial visual presentation. *NeuroImage*. 2010:49(2):1857–1867.

Ma J, Liu C, Chen X. Emotional modulation of conflict processing in the affective domain: evidence from event-related potentials and event-related spectral perturbation analysis. *Sci Rep*. 2016:6(1):1–10.

Mayer K, Krylova M, Alizadeh S, Jamalabadi H, Van Der Meer J, Vester JC, Naschold B, Schultz M, Walter M. Nx4 reduced susceptibility to distraction in an attention modulation task. *Frontiers in Psychiatry*. 2021:12:746215.

Meeren HK, van Heijnsbergen CC, de Gelder B. Rapid perceptual integration of facial expression and emotional body language. *Proc Natl Acad Sci*. 2005:102(45):16518–16523.

Mello M, Dupont L, Engelen T, Acciarino A, de Borst AW, de Gelder B. The influence of body expression, group affiliation and threat proximity on interactions in virtual reality. *Current Research in Behavioral Sciences*. 2022:3:100075.

Michida N, Hayashi M, Hori T. Comparison of event related potentials with and without hypnagogic imagery. *Psychiatry Clin Neurosci*. 1998:52(2):145–147.

Mobbs D, Kim JJ. Neuroethological studies of fear, anxiety, and risky decision-making in rodents and humans. *Curr Opin Behav Sci*. 2015:5:8–15.

Monti A, Aglioti SM. Flesh and bone digital sociality: on how humans may go virtual. *Br J Psychol*. 2018:109(3):418–420.

Oostenveld R, Fries P, Maris E, Schoffelen J-M. FieldTrip: open source software for advanced analysis of MEG, EEG, and invasive electrophysiological data. *Computational Intelligence and Neuroscience*. 2011:2011:156869.

Parsons TD, Gaggioli A, Riva G. Virtual reality for research in social neuroscience. *Brain Sciences*. 2017:7(12):42.

Pellencin E, Paladino MP, Herbelin B, Serino A. Social perception of others shapes one's own multisensory peripersonal space. *Cortex*. 2018:104:163–179.

Perry A, Rubinsten O, Peled L, Shamay-Tsoory SG. Don't stand so close to me: a behavioral and ERP study of preferred interpersonal distance. *NeuroImage*. 2013:83:61–769.

Pilia N, Nagel C, Lenis G, Becker S, Doessel O, Loewe A. ECGdelian open source ECG delineation toolbox for MATLAB. *SoftwareX*. 2021:13:100639.

Qi S, Hassabis D, Sun J, Guo F, Daw N, Mobbs D. How cognitive and reactive fear circuits optimize escape decisions in humans. *Proc Natl Acad Sci*. 2018:115(12):3186–3191.

Riem MM, Kunst LE, Steenbakkers FD, Kir M, Sluijtman A, Karreman A, Bekker MH. Oxytocin reduces interpersonal distance: examining moderating effects of childrearing experiences and interpersonal context in virtual reality. *Psychoneuroendocrinology*. 2019:108:102–109.

Roelofs K, Hagenaars MA, Stins J. Facing freeze: social threat induces bodily freeze in humans. *Psychol Sci*. 2010:21(11):1575–1581.

Ruggiero G, Rapuano M, Cartaud A, Coello Y, Iachini T. Defensive functions provoke similar psychophysiological reactions in reaching and comfort spaces. *Sci Rep*. 2021:11(1):1–12.

Seinfeld S, Bergstrom I, Pomes A, Arroyo-Palacios J, Vico F, Slater M, Sanchez-Vives MV. Influence of music on anxiety induced by fear of heights in virtual reality. *Front Psychol*. 2016:6:1969.

Seinfeld S, Zhan M, Poyo-Solanas M, Barsuola G, Vaessen M, Slater M, Sanchez-Vives MV, de Gelder B. Being the victim of virtual

abuse changes default mode network responses to emotional expressions. *Cortex*. 2021:135:268–284.

Serino A. Peripersonal space (PPS) as a multisensory interface between the individual and the environment, defining the space of the self. *Neurosci Biobehav Rev*. 2019:99:138–159.

Stekelenburg JJ, de Gelder B. The neural correlates of perceiving human bodies: an ERP study on the body-inversion effect. *Neuroreport*. 2004:15(5):777–780.

Stins JF, Roelofs K, Villan J, Kooijman K, Hagenaars MA, Beek PJ. Walk to me when I smile, step back when I'm angry: emotional faces modulate whole-body approach–avoidance behaviors. *Exp Brain Res*. 2011:212(4):603–611.

Stolz C, Endres D, Mueller EM. Threat-conditioned contexts modulate the late positive potential to faces—a mobile EEG/virtual reality study. *Psychophysiology*. 2019:56:e13308.

Sulpizio S, Grecucci A, Job R. Tune in to the right frequency: theta changes when distancing from emotions elicited by unpleasant images and words. *Eur J Neurosci*. 2021:53(3):916–928.

Terburg D, Scheggia D, Del Rio RT, Klumpers F, Ciobanu AC, Morgan B, Montoya ER, Bos PA, Giobellina G, van den Burg EH. The basolateral amygdala is essential for rapid escape: a human and rodent study. *Cell*. 2018:175(3):723–735.

Tieri G, Gioia A, Scandola M, Pavone EF, Aglioti SM. Visual appearance of a virtual upper limb modulates the temperature of the real hand: a thermal imaging study in immersive virtual reality. *Eur J Neurosci*. 2017:45(9):1141–1151.

Van Heijnsbergen C, Meeren H, Grezes J, de Gelder B. Rapid detection of fear in body expressions, an ERP study. *Brain Res*. 2007:1186:233–241.

Vieira JB, Pierzchajlo SR, Mitchell DG. Neural correlates of social and non-social personal space intrusions: role of defensive and peripersonal space systems in interpersonal distance regulation. *Soc Neurosci*. 2020:15(1):36–51.

Weeks JW, Zoccola PM. "having the heart to be evaluated": the differential effects of fears of positive and negative evaluation on emotional and cardiovascular responses to social threat. *Journal of Anxiety Disorders*. 2015:36:115–126.

Wendt J, Löw A, Weymar M, Lotze M, Hamm AO. Active avoidance and attentive freezing in the face of approaching threat. *NeuroImage*. 2017:158:196–204.